

Direct Observation of Charge Order in Triangular Metallic AgNiO_2 by Single-crystal Resonant X-ray Scattering

G.L. Pascut^{1,2}, R. Coldea¹, P.G. Radaelli¹, A. Bombardi³, G. Beutier³, I.I. Mazin⁴, M.D. Johannes⁴, and M. Jansen⁵

¹*Clarendon Laboratory, University of Oxford, Parks Road, Oxford OX1 3PU, United Kingdom*

²*H.H. Wills Physics Laboratory, University of Bristol, Tyndall Avenue, Bristol, BS8 1TL, United Kingdom*

³*Diamond Light Source Ltd., Harwell Science and Innovation Campus, Didcot, Oxfordshire, OX11 0DE, United Kingdom*

⁴*Code 6393, Naval Research Laboratory, Washington, D.C. 20375*

⁵*Max-Planck Institut für Festkörperforschung, Heisenbergstrasse 1, D-70569 Stuttgart, Germany*

(Dated: September 13, 2010)

We report resonant X-ray scattering measurements on a single crystal of the orbitally-degenerate triangular metallic antiferromagnet $2H\text{-AgNiO}_2$ to probe the spontaneous transition to a triple-cell superstructure at temperatures below $T_S = 365$ K. We observe a strong resonant enhancement of the supercell reflections through the Ni K-edge. The empirically extracted K-edge shift between the crystallographically-distinct Ni sites of 2.5(3) eV is much larger than the value expected from the shift in final states, and implies a core-level shift of ~ 1 eV, thus providing direct evidence for the onset of spontaneous honeycomb charge order in the triangular Ni layers. We also provide band-structure calculations that explain quantitatively the observed edge shifts in terms of changes in the Ni electronic energy levels due to charge order and hybridization with the surrounding oxygens.

PACS numbers: 75.25.Dk, 78.70.Ck, 71.45.Lr

Since the discovery of the Verwey transition in 1939 [1], electronic ordering in oxides has been extensively studied, as more evidence progressively emerged of its importance in underpinning phenomena such as metal-insulator transitions, colossal magnetoresistance and possibly high-temperature superconductivity. Orbital ordering (OO) in particular, whereby orbital degeneracy is lifted either by a spontaneous lattice distortion driven by the (cooperative) Jahn-Teller (JT) effect [2], or by similar orbital physics [3], has become a cornerstone of our understanding of oxides. This was hitherto considered ubiquitous in both band and Mott insulators containing “JT active” ions. For this reason, the recent proposal [4] of a radically different type of electronic ordering in the weakly metallic $2H\text{-AgNiO}_2$ came initially as a surprise. In this scenario, orbital degeneracy at JT-active low-spin Ni^{3+} would be lifted through *charge disproportionation and charge ordering* (CO) rather than OO, in sharp contrast with the closely related (but insulating) nickelate NaNiO_2 [5], a rather conventional JT system. Although CO was observed before, e.g. at the simultaneous metal-insulator and magnetic ordering transition in rare-earth perovskite nickelates [6, 7], elucidating the physics of $2H\text{-AgNiO}_2$ is crucial in establishing a pure CO (decoupled from magnetic ordering [8]) as an alternative paradigm to the Jahn-Teller mechanism in “weakly” metallic systems close to the Mott transition [4, 9], which *remain metallic* in the CO phase. Although the original clue for CO was from the magnetic structure below $T_N = 19.7$ K, the primary indication was *structural*, and relied on an accurate neutron refinement of an oxygen breathing mode around the different Ni sites (Fig. 1b) in the $\sqrt{3}a_0 \times \sqrt{3}a_0 \times c$ supercell structure at $T < T_S = 365$

K. The pattern of charges (“honeycomb” CO - see Fig. 1a) and the amount of charge (formal valence) on each site can be estimated by analysing the Ni-O bond lengths through the so-called Bond Valence Sum (BVS) method [10], which yields $\text{Ni}1^{2.42+}$ and $\text{Ni}2,3^{3.07+}$, see Fig. 1b), values that are fairly typical of amounts of charge disproportionation in strongly charge-ordered systems. The CO scenario was also supported by band structure calculations in the Local Density Approximation (LDA) [4]. Nonetheless, obtaining direct experimental evidence of CO *independently* of the pure structural signature is of crucial importance in strengthening the foundations of this new oxide phenomenology.

Here we present resonant Ni-K-edge x-ray scattering data on a single crystal of $2H\text{-AgNiO}_2$ to probe directly the electronic order at the Ni sites. This technique has been widely employed in the past to explore charge and orbital order [11] because of its sensitivity to subtle differences in the electronic environments. In particular, Ni K-edge resonant scattering probes primarily dipole-allowed transitions from the core $1s$ levels, which shift in response to the amount of charge on the ion, to the empty $4p$ band, which is strongly sensitive to changes in the coordination environment. From our data we extract in an unbiased way the anomalous scattering factors of the different Ni sites. By comparing the experimental results with band structure calculations, we show that the $4p$ level shift accounts for just over a half of the edge shift, implying a core-level shift of ~ 1 eV that provides direct evidence of honeycomb CO. These results are also quantitatively consistent with the amount of charge disproportionation predicted by LDA calculations.

Our sample was a small single-crystal platelet of $2H\text{-}$

AgNiO₂ of diameter $\sim 70\mu\text{m}$ in the ab plane and thickness $\sim 20\mu\text{m}$, extracted from a polycrystalline batch[12]. A full single-crystal X-ray diffraction pattern collected at 300 K using an Oxford Diffraction Mo-source diffractometer confirmed the hexagonal unit cell found previously (space group P6₃22 with $a = b = \sqrt{3}a_0 = 5.0908(1)\text{ \AA}$, $c = 12.2498(1)\text{ \AA}$) where supercell peaks are indexed by (h, k, l) with $h - k = 3n + 1$ or $3n + 2$ and correspond to the oxygen breathing order pattern shown in Fig. 1b). Synchrotron resonant X-ray diffraction (RXD) was performed at the Diamond Light Source in Didcot, UK on beamline I16 operated with a Si (111) double-crystal monochromator ($\Delta E/E \approx 10^{-4}$ at 8.35 keV). The azimuth of each supercell reflection was chosen such that the incident polarisation lay as close as possible to the ab plane of the crystal (see below). The sample temperature was controlled via a nitrogen gas flow. Intensities were collected by a 2D Pilatus detector and a typical intensity map for a supercell Bragg reflection is shown in Fig. 2 top-left inset. Total peak intensities were extracted by integrating the counts over rocking-curve scans around the peak position. After all corrections [13], the off-resonance structure factors squared $|F|^2$ at 300 K for all measured main peaks, as well as supercell peaks agreed very well with the calculated values, see Fig. 1c-d), enabling us to convert scattering intensities into $|F|^2$ in absolute units.

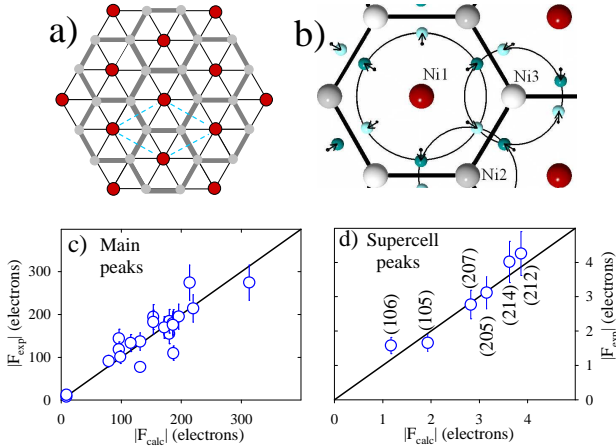


FIG. 1: (color online) a) Schematic of the honeycomb CO in the triangular lattice: red (dark) balls are electron-rich Ni1 sites nested inside a honeycomb (thick contour) of electron-depleted Ni2,3 sites (gray balls). The dashed rhombus is the CO supercell. b) Oxygen breathing mode around electron-rich and -depleted Ni sites. c) and d) Observed vs. calculated off-resonance (8.3 keV) $|F|^2$ for main and supercell peaks.

Fig. 2 shows the energy-dependent $|F|^2$ for three supercell reflections (out of the 6 measured), which are representative of the different types of resonant responses. In particular the (109) peak is entirely due to anomalous scattering from Ni as it is practically absent off-

resonance. The middle and bottom panels show the (105) and (205) supercell peaks, which have a sizeable oxygen contribution, as evidenced by the off-edge scattering.

In the dipolar approximation the atomic scattering factor near the K-edge absorption energy E_A is

$$f(Q, E) = f^0(Q) + f'(E) + if''(E), \quad (1)$$

where f^0 is the conventional (Thomson) Q -dependent scattering factor [14], and f' , f'' are the real and imaginary parts of the anomalous scattering factor, respectively. In essence, the rich structures observed in Fig. 2 are due to the fact that E_A of the electron-rich Ni1 is slightly different from that of electron-depleted Ni2,3 providing a strong energy-dependent contrast between the two sites. More specifically, the $|F|^2$ for the (109), (105) and (205) peaks can be written as

$$|F(Q, E)|^2 = 3 \left[\mp A_Q f_O^0 / \sqrt{3} + \Delta f_{\text{Ni}}^0 + \Delta f_{\text{Ni}}' \right]^2 + 3 \Delta f_{\text{Ni}}''^2, \quad (2)$$

where the upper sign applies for (109) and (105), and lower sign for (205). The dominant term off-resonance is $A_Q f_O^0$, the energy-independent structure factor for the oxygen breathing displacement order, which is weak for supercell peaks like (109) and strong for (205) and (105). In contrast, the terms $\Delta f_{\text{Ni}}' = f_{\text{Ni1}}'(E) - f_{\text{Ni3}}'(E)$ and $\Delta f_{\text{Ni}}'' = f_{\text{Ni1}}''(E) - f_{\text{Ni3}}''(E)$ have the same value for different reflections but are strongly energy-dependent and are due to the contrast between the anomalous atomic factors for Ni1 inside the honeycomb and Ni3 on the honeycomb (contributions from Ni2 cancel by symmetry). The remaining term $\Delta f_{\text{Ni}}^0 = f_{\text{Ni1}}^0 - f_{\text{Ni3}}^0$ is the Thomson charge contrast, and can essentially be neglected since the difference in electronic density is small and highly delocalised. All contributions to eq. (2) cancel in the high-temperature phase above T_S , since all Ni sites become equivalent and the oxygens are not displaced from their ideal positions. This can be shown by plotting the intensity of different superlattice reflections as a function of temperature (top-right inset of Fig. 2). These data also show that the order parameter obtained from the purely-resonant peak (109) (“CO order parameter”) is essentially the same as extracted from the intensity of the (212) supercell peak, which has comparable contributions from both Ni CO and Oxygen displacements, indicating that, as expected, CO and displacements are strongly coupled and both go to zero together at T_S .

It is important to point out that, because of the asphericity of the electron density, f' and f'' in eq. (1) are in general not scalar quantities, but depend on the orientation of the incident and scattered polarisations with respect to the crystallographic axes, as expressed through the general tensor relation $f(E) = \sum_{\alpha, \beta} \hat{f}^{\alpha\beta} \epsilon_\alpha \epsilon'_\beta$ (valid for both f' and f''), where ϵ and ϵ' are the incident and scattered polarisation vectors. In 2H-AgNiO₂ the local three-fold symmetry axis at *each* Ni site restricts

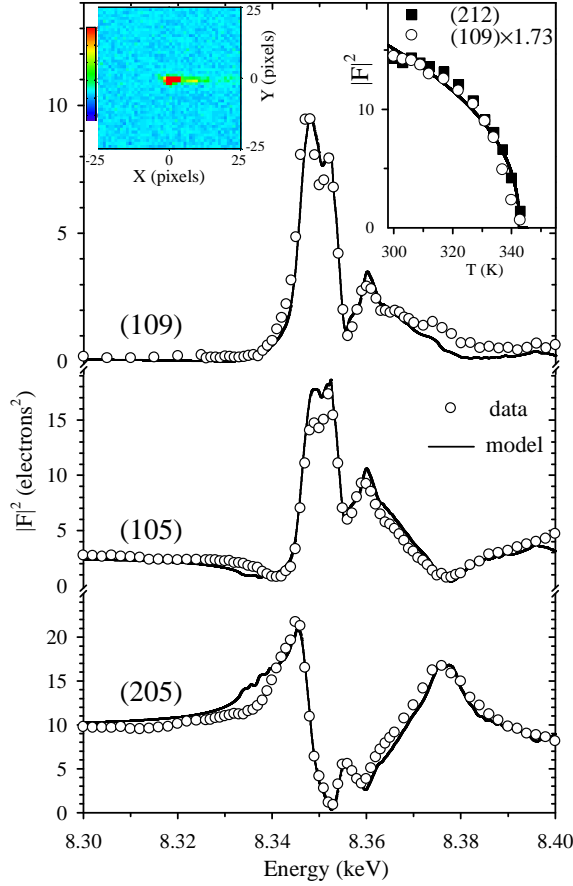


FIG. 2: (color online) Energy-dependent intensity of three supercell reflections at 300 K near the Ni K-edge. (solid lines are model calculations eq. (2)). Top-left inset: example of raw 2D pixelated area detector data for (109) near resonance. The horizontal (vertical) angular coverage is $\approx 1^\circ$ (0.7°). Top-right inset: Temperature-dependence of peak intensities near resonance (8.347 keV) for (109), dominated by Ni charge order (open symbols, scaled) and for (212), with contributions from both Ni CO and Oxygen displacements (solid squares). Solid line is a guide to the eye. The transition temperature is offset with respect to the specific heat and neutron diffraction value [4] (343(1) K vs. 365(5) K), probably due to X-ray beam heating effects.

\hat{f}' and \hat{f}'' to have a diagonal form in the orthogonal reference frame xyz where $x \parallel a$ and $z \parallel c$, such that $\hat{f} = \begin{bmatrix} f_{\perp} & 0 & 0 \\ 0 & f_{\perp} & 0 \\ 0 & 0 & f_{\parallel} \end{bmatrix}$, where \parallel is along the c axis and \perp is in the ab plane. Because of our choice of azimuth, the incident polarisation was always nearly *perpendicular* to the c axis. Consequently, our data were sensitive only to $\sigma\sigma$ -type scattering [15] and we can employ the scalar relation in eq. (2) with f' and f'' being the in-plane components f'_{\perp} and f''_{\perp} of the anomalous scattering tensors.

Remarkably, the complex multiple-peak structure of the spectra in Fig. 2 can be reproduced quantitatively (in absolute units) by a model (solid lines) based on an

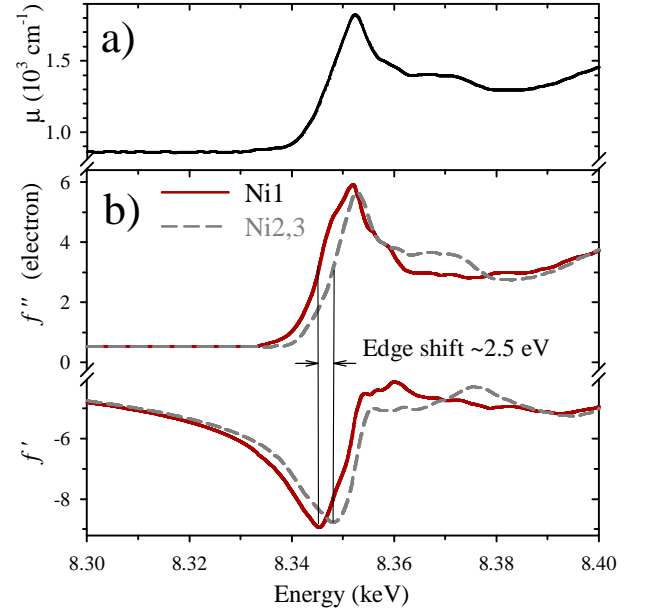


FIG. 3: (color online) a) Energy-dependence of the absorption coefficient μ obtained from transmission data. b) Energy-dependence of the empirically-extracted real and imaginary anomalous atomic scattering factors for Ni1 (solid line) and Ni2,3 (dashed line) obtained from a best fit to measured spectra as shown in Fig. 2.

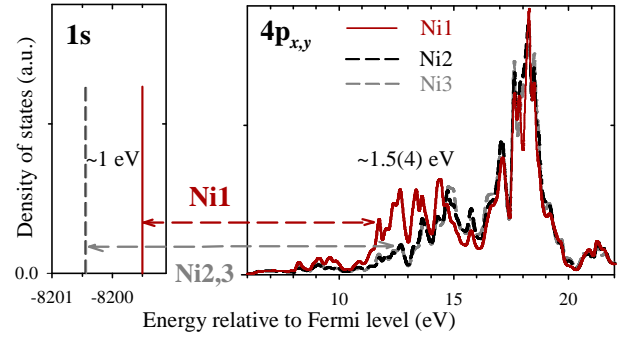


FIG. 4: (color online) LDA calculation of density of states (DOS) for the initial and final electron states in the transition $1s \rightarrow 4p_{x,y}$ (horizontal dashed arrows) probed by the present resonant Ni K-edge scattering experiments. Solid/dashed curves show the DOS for electron-rich/depleted Ni1/Ni2,3 sites. The combined effect is a predicted transition energy shift of 2.5(4) eV higher for Ni2,3 compared to Ni1, in excellent agreement with the experiment.

unbiased reconstruction of the atomic scattering factors for the Ni1 and Ni2,3 (Fig. 3b). In this analysis we assumed identical scattering factors for both Ni sites on the honeycomb $f_{\text{Ni2}} = f_{\text{Ni3}}$ as their first-neighbor environments (Ni-O bond lengths and angles) are identical [4]. The two functions $f''_{\text{Ni1}}(E)$ and $f''_{\text{Ni3}}(E)$ were optimised iteratively to best match the observed spectra, under the constraints of a given *average* $f''_{\text{fu}} = f''_{\text{Ag}}(E) + 2f''_{\text{O}}(E) + [f''_{\text{Ni1}}(E) + 2f''_{\text{Ni3}}(E)]/3$ per formula

unit, which is related to the linear absorption coefficient (see above) via [16] $\mu(E) = (2Zhc r_e / V_{uc} E) f''_{fu}(E)$, where $Z = 6$ is the number of formula units per unit cell of volume V_{uc} , hc/E is the x-ray wavelength and r_e is the classical electron radius. The *real* parts of the scattering factors f' in eq. (2) were obtained via the Kramers-Kronig (KK) relation [16, 17] from the imaginary parts f'' , such that the *individual* anomalous scattering factors obey the KK relation. Starting values for the profiles $f''_{Ni1,3}(E)$ were obtained by subtracting the intensities $|F(\mathbf{Q}, E)|^2$ such as in Fig. 2 for various reflections (with the energy independent terms $\mp A_{\mathbf{Q}} f_O^0 / \sqrt{3} + \Delta f_{Ni}^0$ replaced by their measured values off-resonance) to give the difference $f'_{Ni1}(E) - f'_{Ni3}(E)$. After inserting this back into eq. (2) one obtains the modulus $|f''_{Ni1}(E) - f''_{Ni3}(E)|$. Combining this with the constraint for the sum $f''_{Ni1}(E) + 2f''_{Ni3}(E)$ yields a few possibilities for starting profiles for the two functions $f''_{Ni1,3}(E)$ (this is due to the sign uncertainty), but with only one set satisfying all the constraints above. The best parameterization of the data (solid lines in Fig. 2) is obtained for the atomic scattering factors in Fig. 3b), which show a clear energy shift of the edge of $+2.5(3)$ eV and some subtle differences at higher energy [18]. The sign of the energy shift is fully consistent with an electron-rich Ni1 site [19, 20] and is uniquely determined from the data. In addition, the absolute scaling of the peak intensities ensures an accurate and reliable determination of the *magnitude* of the edge shift.

Edge shifts are often taken as directly proportional to changes in the formal valence of the ion. For octahedral Ni, the proportionality constant is ~ 0.66 electrons/eV [19], so an edge shift of 2.5 eV corresponds to a disproportionation of ~ 1.65 electrons, in very good agreement with the expected CO scenario of $Ni1^{2+}$ and $Ni2,3^{3.5+}$ [4]. However, the initial- and final-states contributions to the edge shift are typically of similar magnitudes, while only the former are *directly* related to charge ordering. To estimate the core-level shifts, we determined the positions of the $4p$ final states from LDA band-structure calculations [4]. These are completely independent of the details of the electronic structure near the Fermi energy, and are therefore reliable and unaffected by assumptions made about electronic correlations. The $4p_{x,y}$ (degenerate) densities of states are shown in Fig. 4 (only these bands are probed in the present experiments). The Ni1 and Ni2,3 $4p$ bands are shifted by ~ 1.5 eV, well short of the $2.5(3)$ eV we observed experimentally, providing clear evidence that a core level shift of ~ 1 eV is required to reproduce the data. Further insight can be gained by extracting directly the positions of the core $1s$ levels on the Ni1 and Ni2,3 sites from the LDA calculations (left panel, Fig. 4), which indeed differ by ~ 1 eV. This demonstrates that the LDA calculations are quantitatively consistent with the resonant scattering experiment, and provides strong evidence of honeycomb CO with an amount of charge disproportionation in agreement with LDA.

In summary, we have reported Ni-K-edge resonant X-ray scattering measurements on a single-crystal of the triangular-lattice metal $2H\text{-AgNiO}_2$ which undergoes a spontaneous ordering transition that we have previously interpreted in terms of charge disproportionation and honeycomb charge order. We have observed a large resonant effect on the superstructure reflections. The rich energy-dependent structure can be quantitatively accounted for by interference scattering from the electron-rich and -depleted Ni sites. By comparing our data with electronic structure calculations we determined a core-level shift of ~ 1 eV between Ni sites, providing clear, direct and quantitative evidence of charge ordering.

We acknowledge support from EPSRC UK and a studentship from the University of Bristol and Potter foundation (GLP). We thank E. Wawrzyńska and M. Brunelli for characterising the polycrystalline sample on Beamline ID31 at the ESRF.

-
- [1] E.J.W. Verwey, *Nature* **144**, 327 (1939).
 - [2] H. Jahn and E. Teller, *Proc. R. Soc. London Ser. A* **161**, 220 (1937).
 - [3] K.I. Kugel and D.I. Khomskii, *Sov. Phys. Usp.* **25**, 231 (1982).
 - [4] E. Wawrzyńska *et al.*, *Phys. Rev. Lett.* **99**, 157204 (2007); *ibid* *Phys. Rev. B* **77**, 094439 (2008).
 - [5] E. Chappel *et al.*, *Eur. Phys. J. B* **17**, 615 (2000).
 - [6] J.A. Alonso *et al.*, *Phys. Rev. Lett.* **82**, 3871 (1999).
 - [7] U. Staub *et al.*, *Phys. Rev. Lett.* **88**, 126402 (2002).
 - [8] S. Lee, R. Chen, and L. Balents, *arXiv:1008.2373* (2010).
 - [9] I.I. Mazin *et al.*, *Phys. Rev. Lett.* **98**, 176406 (2007).
 - [10] I. D. Brown, in *Structure and Bonding in Crystals*, ed. M. O'Keefe and A. Navrotsky (Academic, New York, 1981), **2**, pp. 130.
 - [11] Y. Murakami *et al.*, *Phys. Rev. Lett.* **80**, 1932 (1998).
 - [12] T. Sörgel and M. Jansen, *Z. Anorg. Allg. Chem.* **631**, 2970 (2005); *J. Solid State Chem.* **180**, 8 (2007).
 - [13] Raw intensities were corrected for Debye-Waller factor (using atomic displacements from [12]), Lorenz factor, and absorption using a numerical beam-path integration routine for a disk-shaped sample with effective dimensions refined against the measured (off-resonance) intensity ratios of several main (hkl) reflections with $h - k = 3n$ and l odd where Ni contributions to F cancel out. The linear absorption coefficient $\mu(E)$ in Fig. 3a) was extracted from the measured transmission spectrum through a thin layer of powder distributed on kapton tape. Off-resonance the analytic approximation for $f'(E)$ and $f''(E)$ was used [16].
 - [14] International Tables for Crystallography, ed. A.J.C. Wilson, vol. C, p. 182 and 500 (1992).
 - [15] For the case of no analyser (as in the present experiments) eq. (2) becomes the sum (we drop the E and Q dependence for brevity) $|F|^2 = |F|_{\sigma\sigma}^2 + |F|_{\sigma\pi}^2$, where $|F|_{\sigma\sigma}^2 = 3 [\mp A_{\mathbf{Q}} f_O^0 / \sqrt{3} + \Delta f^0 + \Delta f'_{\perp} + \gamma^2 (\Delta f'_{\parallel} - \Delta f'_{\perp})]^2 + 3 [\Delta f''_{\perp} + \gamma^2 (\Delta f''_{\parallel} - \Delta f''_{\perp})]^2$ and $|F|_{\sigma\pi}^2 = 3(\gamma\gamma')^2 [(\Delta f'_{\parallel} - \Delta f'_{\perp})^2 + (\Delta f''_{\parallel} - \Delta f''_{\perp})^2]$ where

the difference terms are $\Delta f''_{\perp} = f''_{\perp}(\text{Ni1}) - f''_{\perp}(\text{Ni3})$ and so on. Here γ, γ' are projections onto the crystal \mathbf{c}^* -axis of the incident x-ray beam polarization vector $\boldsymbol{\sigma}$ (which is perpendicular to the scattering plane) and of the unit vector $\boldsymbol{\pi}$ (within the scattering plane and \perp to \mathbf{k}_f).

- [16] C.T. Chantler, J. Phys. Chem. Ref. Data **24**, 71 (1995).
- [17] I.J. Pickering *et al.*, J. Am. Chem. Soc. **115**, 6302 (1993).
- [18] The assumption $f_{\text{Ni2}} = f_{\text{Ni3}}$ was further justified by the

observed agreement with the data at supercell peaks with l even, (106), where both Ni2 and Ni3 contribute.

- [19] A. N. Mansour and C. A. Melendres, J. Phys. Chem. A **102**, 65 (1998); J. Phys. IV **7**, C2-1171 (1997).
- [20] T. A. Carlson, in *Photoelectron and Auger Spectroscopy* (New York, Plenum, 1975), p. 165.